Queiroz et al. Journal of Neuroinflammation (2020) 17:96
https://doi.org/10.1186/s12974-020-01763-y

Journal of Neuroinflammation

RESEARCH Open Access

Vitamin B_{12} is neuroprotective in experimental pneumococcal meningitis through modulation of hippocampal DNA methylation

Karina Barbosa de Queiroz[1], Vanessa Cavalcante-Silva[2], Flávia Lombardi Lopes[3], Gifone Aguiar Rocha[4], Vânia D'Almeida[2] and Roney Santos Coimbra[1*]

Abstract

Background: Bacterial meningitis (BM) causes apoptotic damage to the hippocampus and homocysteine (Hcy) accumulation to neurotoxic levels in the cerebrospinal fluid of children. The Hcy pathway controls bioavailability of methyl, and its homeostasis can be modulated by vitamin B_{12}, a cofactor of the methionine synthase enzyme. Herein, the neuroprotective potential and the underlying mode of action of vitamin B_{12} adjuvant therapy were assessed in an infant rat model of BM.

Methods: Eleven-day old rats were intracysternally infected with *Streptococcus pneumoniae* serotype 3, or saline, treated with B_{12} or placebo, and, 24 h after infection, their hippocampi were analyzed for apoptosis in the dentate gyrus, sulfur amino acids content, global DNA methylation, transcription, and proximal promoter methylation of candidate genes. Differences between groups were compared using 2-way ANOVA followed by Bonferroni post hoc test. Correlations were tested with Spearman's test.

Results: B_{12} attenuated BM-induced hippocampal apoptosis in a Hcy-dependent manner ($r = 0.80$, $P < 0.05$). BM caused global DNA hypomethylation; however, B_{12} restored this parameter. Accordingly, B_{12} increased the methylation capacity of hippocampal cells from infected animals, as inferred from the ratio *S*-adenosylmethionine (SAM):*S*-adenosylhomocysteine (SAH) in infected animals. BM upregulated selected pro-inflammatory genes, and this effect was counteracted by B_{12}, which also increased methylation of CpGs at the promoter of *Ccl3* of infected animals.

Conclusion: Hcy is likely to play a central role in hippocampal damage in the infant rat model of BM, and B_{12} shows an anti-inflammatory and neuroprotective action through methyl-dependent epigenetic mechanisms.

Keywords: Meningitis, Neuroprotection, Vitamin B_{12}, Epigenetics, Homocysteine, DNA methylation

* Correspondence: roney.coimbra@fiocruz.br
[1]Neurogenômica/Imunopatologia, Instituto René Rachou (IRR), Fundação Oswaldo Cruz (FIOCRUZ), Av. Augusto de Lima, 1715, Belo Horizonte, MG CEP 30190-002, Brazil
Full list of author information is available at the end of the article

Background

The estimated incidence of bacterial meningitis (BM) is 0.7–0.9/100,000 people per year in developed countries and can reach values up to 10–40/100,000 in some African countries [1]. The most common etiologic agents of BM are *Streptococcus pneumoniae* (pneumococcus), *Neisseria meningitidis,* and *Haemophilus influenzae* type b (Hib). Since the advent of anti-Hib vaccine in the late 90s, pneumococcus has become the most frequent cause of non-epidemic BM among children older than 1 year of age [2, 3]. Pneumococcal meningitis is associated with the highest mortality (30%) and morbidity rates in BM [4]. Between 30 and 50% of survivors develop permanent neurological sequelae, including sensory-neural deafness, cognitive deficits, and sensory-motor disabilities, seizures, and cerebral palsy [5–8].

BM is characterized by intense granulocytic inflammation within the subarachnoid and ventricular spaces, extending into the perilymphatic space of the inner ear. This granulocytic inflammation results in extensive neuronal damage, primarily in the brain cortex (CX) and hippocampus (HC). In CX, the main lesion is acute neuronal necrosis, while apoptosis is the predominant form of cell injury in HC (reviewed in [9]). HC cells undergoing apoptosis are mostly post mitotic neurons and progenitor cells distributed along the inner granule cell layer of the dentate gyrus [10, 11].

During the acute phase of BM, dramatic changes in multiple gene expression pattern may occur in CX and HC, as reported by Coimbra et al. [12]. These changes have a fundamental role regulating neurodegeneration and neuroregeneration processes, in an attempt to recover the cognitive function in BM survivors. The HC is particularly susceptible to structural, functional, and neurogenic rearrangements in response to environmental stimuli [13–15]. Several research groups have reported evidence that these alterations are regulated by epigenetic processes, defined as inheritable states of gene activity not based on changes in DNA sequence [16–18]. One of the major epigenetic mechanisms is DNA cytosine methylation [19]. Alterations in DNA methylation have been linked to human diseases, such as cancer and several neurological disorders, suggesting an important role for this epigenetic process in brain function [20]. However, the intrinsic regulatory programs and environmental factors that may modulate neuroinflammation remain unclear.

Disturbances in methyl bioavailability are associated with neurological disorders. *S*-adenosylmethionine (SAM or AdoMet) is the main cellular methyl donor involved in DNA, RNA, and histone methylation that may modulate gene expression via epigenetic mechanisms [21]. SAM (or AdoMet) is synthesized from ATP and methionine, which can be either dietary or formed by methylation of homocysteine (Hcy), using a methyl group of 5-methyltetrahydrofolate in a cobalamin (vitamin B_{12})-dependent reaction [22]. Methylation reactions generate *S*-adenosylhomocysteine (SAH or AdoHcy), a potent inhibitor of methyltransferases AdoMet-dependent. SAH (or AdoHcy) can be hydrolyzed to adenosine and Hcy; Hcy, in turn, can be remethylated by methionine synthase or withdrawn from the methylation cycle through conversion to cysteine (Cys), in a two-step transsulfuration pathway that requires vitamin B_6 (Fig. 1). The reduction in SAM:SAH ratio is considered an indicator of decreased methylation capacity of the cells [24]; also, plasma Hcy levels can be lowered with B vitamin supplementation [25]. Our group has shown that Hcy levels in cerebrospinal fluid (CSF) are significantly higher in children with acute BM than in children with enteroviral meningitis or without infection in the central nervous system (CNS), suggesting a role of Hcy in BM pathophysiology [26]. Therefore, the hypothesis of this study is that the imbalance in the homeostasis of the sulfur amino acids could play a role in the pathophysiology of BM and that adjuvant therapy with vitamin B_{12} might increase promoter methylation of pro-inflammatory genes, leading to their downregulation, thus contributing to neuroprotection of progenitor cells and post mitotic neurons in the hippocampal dentate gyrus.

Methods

Animal model and experimental design

The experiments were conducted using a well-established experimental BM model in infant rats [27]. At postnatal day 11, Wistar rats (20 ± 2 g) were infected by intracisternal injection of 10 μL saline (0.85% NaCl) containing ~ 2×10^6 cfu/mL of *S. pneumoniae* (serotype 3, strain 38/12 MEN from the certified bacterial collection of the Ezequiel Dias Foundation). Animals in the control groups were sham-infected by intracisternal injection of 10 μL of sterile saline. Infected and sham-infected animals were separated into four groups according to the treatment received: 10 μL of intramuscular vitamin B_{12} (Merck, Kenilworth, NJ; 6.25 mg/kg) ($N = 10$ infected, vitamin B_{12}; 10 sham-infected, vitamin B_{12}) or 10 μL of intramuscular saline ($N = 10$ infected, saline; 10 sham-infected, saline). Vitamin B_{12} or placebo was administered at 3 and 18 h post-infection. B_{12} dose and treatment paradigm were defined empirically. No other doses were tested. At the time the first dose was administered, infected animals presented with fever and neck stiffness.

Eighteen hours after infection, all rats were weighed and clinically assessed by the following score system: 1 for comatose animals, 2 for rats that do not turn upright after positioning on the back, 3 for animals that turn within 30 s, 4 for animals that turn within less than 5 s, and 5 for rats with normal activity. Infection was

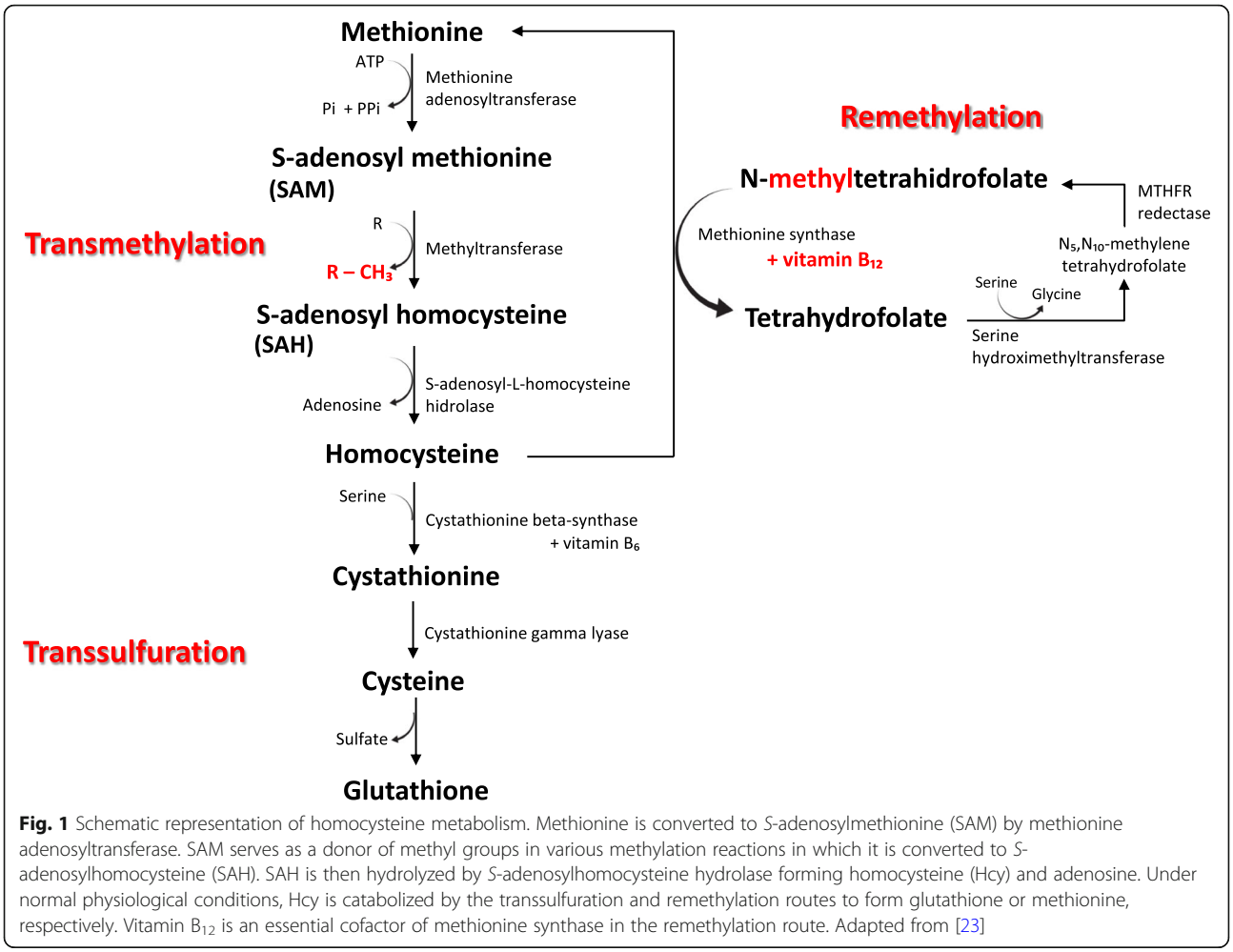

Fig. 1 Schematic representation of homocysteine metabolism. Methionine is converted to *S*-adenosylmethionine (SAM) by methionine adenosyltransferase. SAM serves as a donor of methyl groups in various methylation reactions in which it is converted to *S*-adenosylhomocysteine (SAH). SAH is then hydrolyzed by *S*-adenosylhomocysteine hydrolase forming homocysteine (Hcy) and adenosine. Under normal physiological conditions, Hcy is catabolized by the transsulfuration and remethylation routes to form glutathione or methionine, respectively. Vitamin B_{12} is an essential cofactor of methionine synthase in the remethylation route. Adapted from [23]

documented by quantitative culture of 10 μL of CSF, and all animals were treated with 100 mg ceftriaxone/kg of body administered subcutaneously (EMS Sigma Pharma Ltda., São Paulo, Brazil) [27]. Twenty-four hours after infection, rats were euthanized by an intraperitoneal overdose of Ketamine (300 mg/kg) + Xylazine (30 mg/kg) (Syntec, São Paulo, Brazil).

Immediately after euthanasia, animals were perfused via the left cardiac ventricle with 7.5 mL of RNAse-free ice-cold phosphate-buffered saline (PBS). Brains were removed from the skulls and the two hemispheres were divided; the right hemispheres were processed for histopathological assessment. The hippocampus from the left hemispheres were dissected in three segments, one was stored on RNAlater (ThermoFisher, Waltham, MA) (24 h at 4 °C followed by − 80 °C until use), and the two others were snap frozen at − 80 °C to DNA and sulfur amino acids analysis (see Additional file 1).

Brain histopathological analysis

To assess the potential of vitamin B_{12} adjuvant therapy to prevent hippocampal damage caused by BM, brains were evaluated as previously described ($N = 10$) [27, 28]. Briefly, the right hemisphere was fixed in 4% paraformaldehyde (Sigma-Aldrich, St. Louis, MI), embedded in paraffin, and 5-μm thick histological sections were Nissl stained with Cresyl violet. Sections were examined using a × 40 objective.

Neurons of the lower blade of dentate gyrus with morphological changes characteristic of apoptosis (condensed, fragmented nuclei and/or apoptotic bodies) were counted in the largest visual field of four sections for each rat. An average score per animal was calculated from all sections evaluated, applying the following scoring system: 0–5 cells = 0, 6–20 cells = 1 and > 20 cells = 2 [29].

Quantification of sulfur amino acids in hippocampal samples

One third of each hippocampus was homogenized in PBS using a tissue homogenizer (T10 basic IKA, Staufen, Germany). For SAM and SAH measurements, protein and debris were precipitated from total homogenate tissue with $HClO_4$ and centrifuged. Supernatant was then

injected into a column C18 LiChroCart (5 mm, 250 mm, 64 mm). The mobile phase was applied at a flow rate of 1 mL × min^{-1} and consisted of 50 mM sodium phosphate (pH 2.8), 10 mM heptan sulfonate, and 10% acetonitrile. The UV detector had a wavelength of 254 nm. Retention time was 8.7 min for SAH and 13.6 min for SAM, a technique adapted from Blaise et al. [30]. Hcy, Cys, and glutathione (GSH) were quantified by high-performance liquid chromatography (HPLC) through fluorescence detection and isocratic elution. The method developed by Pfeiffer et al. [31] was employed with slight modifications, as follows: column C18 Luna (5 mm, 150 mm, 64.6 mm), mobile phase [0.06 M sodium acetate, 0.5% acetic acid, pH 4.7 (adjusted with acetic acid), 2% methanol], and flow rate of 1.1 mL × min^{-1}. The retention time was 3.6 min for Cys, 5.2 min for Hcy, and 9.0 min for GSH [32]. For reduced GSH quantification, the reducing agent was not added, and the concentrations were calculated.

Total RNA preparation

Total RNA was obtained from hippocampus using a combination of Invitrogen Trizol reagent (ThermoFisher) and chloroform (Merck) for extraction, according to the manufacturer's protocol. Then, total RNA was purified in a column using the miRNeasy Mini Kit (Qiagen, Hilden, Germany) according to the manufacturer's protocol. Total RNA was treated with RNase-Free DNase Set (Qiagen), following the kit's instruction. Total RNA was quantified using the Life Technologies Qubit 2.0 Fluorometer (ThermoFisher). RNA integrity was assessed with Bioanalyzer using the kit RNA 6000 Nano (Agilent Technologies, Waldbronn, Germany).

Real-time quantitative polymerase chain reaction for a selection of genes previously implicated in the pathophysiology of BM and DNA methylation/demethylation

Two hundred nanograms of total RNA were reverse transcribed into cDNA using the Applied Biosystem High Capacity cDNA RT kit (ThermoFisher). mRNA expression was quantified by real-time quantitative PCR using the Applied Biosystem Taqman system (ThermoFisher) and the ABI 7500 Fast Real-Time PCR System. Rat-specific Taqman assays were used to detect *Ccr2* [Chemokine (C-C Motif) Receptor 2] (Rn01637698_s1), *Ccl3* [Chemokine (C-C Motif) Ligand 3] (Rn01464736_g1), *Il1b* (Interleukin 1 beta) (Rn00580432_m1), *Ccl2* [Chemokine (C-C Motif) Ligand 2] (Rn00580555_m1), *Mmp9* (Matrix Metalloproteinase 9) (Rn00579162_m1), *Ocln* (Occludin) (Rn00580064_m1), *Timp1* (Tissue Inhibitor of Metallopreteinase-1) (Rn01430873_g1), *Tjp2* (Tight Junction Protein 2) (Rn01501483_m1), *Il6* (Interleukin 6) (Rn01410330_m1), *Casp3* (Caspase 3) (Rn00563902_m1), *Nfkb* (Rn01399572_m1), *Tnfa* (Tumor Necrosis Factor alpha) (Rn01525859_g1), *Il10* (Interleukin 10) (Rn01483988_g1), *Cxcl1* [Chemokine (C-X-C Motif) Ligand 1] (Rn00578225_m1), *Dnmt3a* (DNA methyltransferase 3 alpha) (Rn01027162_g1), and *Tet1* (Tet methyl cytosine dioxygenase 1) (Rn01428192_m1). Cycle thresholds (Ct) were determined based on the Taqman emission intensity during the exponential phase. Ct data were normalized by *Rplp2* (Ribosomal Protein, Large, P2) (Rn01479927_g1), and *Ppia* (Peptidylprolyl isomerase A) (Rn00690933_m1) expression, which was stably expressed in all experimental groups. The relative gene *expression* was calculated using the $2^{-\Delta\Delta Ct}$ method [33].

DNA preparation

DNA of tissue samples was extracted and purified using The Wizard Genomic DNA Purification Kit (Promega, Madison, WI). Total DNA was quantified using the Life Technologies Qubit 2.0 Fluorometer (ThermoFisher).

Assessment of global DNA methylation

Global DNA methylation was measured using the Methyl Flash Global DNA Methylation (5mC) ELISA Easy Kit (Colorimetric) (EpiGenteK, Farmingdale, NY), according to manufacturer's instructions. Briefly, 100 ng of genomic DNA from hippocampus ($N = 6$ animals per group) were bound to strip-wells specifically treated to have high DNA affinity. The methylated fraction of DNA was detected using capture and detection antibodies and then quantified colorimetrically by reading the absorbance in a micro plate spectrophotometer (450 nm). Data are presented as percentage of methylated DNA (%5mC), where the sample optical density (OD) was divided by the standard curve slope plus the OD of the DNA input.

Assessment of DNA methylation in promoters of inflammatory genes

DNA was digested with the restriction enzyme *AluI* (20 units to 0.5 μg of DNA, 37 °C, 20 h) (ThermoFisher) prior to methylation enrichment. *AluI* recognition sequence (AG^CT) does not contain the CpG dinucleotide [34].

Two hundred and fifty nanograms of total DNA from each sample were processed with Invitrogen MethylMiner Methylated DNA Enrichment Kit (ThermoFisher), following the manufacturer's instructions. Methylated DNA was eluted from beads using high-salt (2 M NaCl) condition. Captured DNA (methylated) and input DNA were quantified by real-time quantitative PCR using the Applied Biosystems SYBR Green system (ThermoFisher) and the ABI 7500 Fast Real-Time PCR System were used to detect the target. Rat-specific primer pairs flanking

proximal promoter regions containing CpG-rich regions and located between two *AluI* recognition sites were designed to *Ccr2* (F 5′ CAAGTGCAGTGCCTAGAGGTT 3′; R 5′ CACCTGTAATTCCAGTTTTAGGG 3′), *Ccl3* (F 5′ GGCTTCAGACACCAGAAGGA 3′; R 5′ GACTGCTGTGGTCTGCCTTAG 3′), and *Il1b* (F 5′ TCTTGGGTTGCTTGATACTGC 3′; R 5′ CATAGC CAGCCTCATGTTGA 3′). The absolute standard curve method was used to quantify the DNA amount, and data were expressed as a percentage of methylated DNA [(captured DNA/input DNA) × 100].

Statistical analysis

Statistical analyses were performed using Graph Pad Prism version 6.0 (GraphPad Software Inc., Irvine, CA). Shapiro-Wilk test was used to verify data distribution. Differences between groups were compared using 2-way ANOVA followed by Bonferroni post hoc test. Correlations were tested with Spearman's test. Differences were considered statistically significant when P values < 0.05.

Results

Adjunctive therapy with B_{12} reduced apoptotic cell counts in the hippocampal dentate gyrus of infant rats with BM

All animals infected with *S. pneumoniae* had BM after 18 h p.i., as evidenced by positive bacterial titers in the CSF (~ 1×10^8 cfu/mL). BM decreased the activity score of the infant rats compared to sham-infected controls (4 vs. 5; $P <$ 0.001). Adjuvant therapy with vitamin B_{12} did not influence bacterial titers and activity scores, but significantly reduced apoptosis in the dentate gyrus inner granular layer of infected animals ($P < 0.01$), unveiling a neuroprotective effect of this potential adjuvant therapy in BM (Fig. 2).

BM activated the sulfur amino acid pathway in the hippocampus

Hcy, Cys, and total and reduced GSH were measured in the opposite hippocampi of the same animals used for histopathology. Hippocampal levels of Hcy and GSH were increased by BM (2-way *ANOVA* $P < 0.01$). However, no effect of B_{12} was observed in these parameters (Table 1). In the infected group treated with B_{12}, a positive correlation was found between hippocampal Hcy concentration and the apoptotic score in the dentate gyrus of the opposite hippocampus ($r = 0.80$, $P < 0.05$). In the infected group receiving placebo, the apoptotic score did not correlate with Hcy concentration.

To evaluate the effect of BM and of the adjuvant therapy with vitamin B_{12} on methyl bioavailability, SAM and SAH were measured in the same hippocampal samples tested for Hcy, Cys, and GSH (Fig. 3). SAM levels were 35% higher in infected rats treated with vitamin B_{12} as compared to infected + saline and sham-infected + B_{12} ($P < 0.05$) (Fig. 3A). Most important, a significant increase in SAM:SAH was observed in infected rats treated with vitamin B_{12} as compared to infected + saline and sham-infected + B_{12} ($P < 0.05$) (Fig. 3C), suggesting an

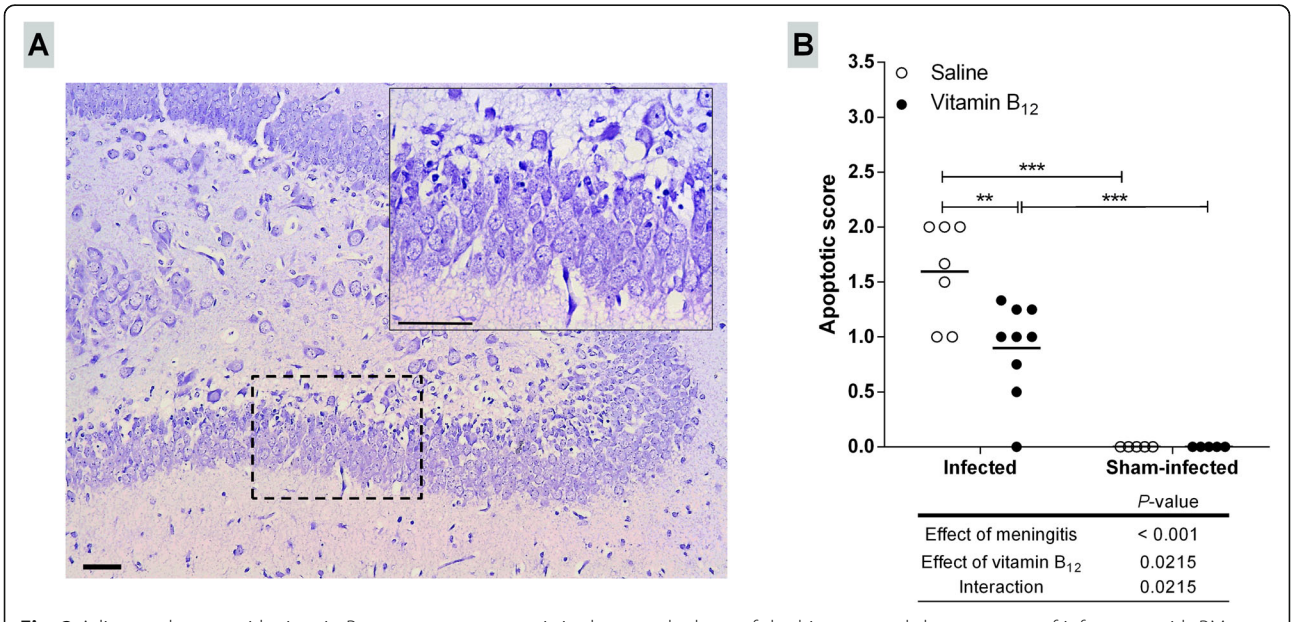

Fig. 2 Adjuvant therapy with vitamin B_{12} attenuates apoptosis in the granular layer of the hippocampal dentate gyrus of infant rats with BM. **a** Nissl-stained histological section showing the hippocampal dentate gyrus (× 100) of an infected animal treated with placebo. The detail shows an amplified section of the lower blade of the granular layer (× 400). Barr = 50 μm. **b** Apoptotic scores. Horizontal bars represent means. The effects of the BM and adjuvant treatment with vitamin B_{12} were compared using a 2-way ANOVA (Bonferroni post hoc test). P values in tables below the graphs refer to the 2-way ANOVA and asterisks refer to the post hoc test. **$P < 0.01$; ***$P < 0.001$

Table 1 Effects of BM and adjuvant therapy with vitamin B_{12} on sulfur amino acids and their metabolites in the hippocampus

	Concentrations in groups (μmol/g of protein)				*P* values (2-way ANOVA)		
	Sh-Sal	Sh-B_{12}	Infect-Sal	Infect-B_{12}	Effect of BM	Effect of vitamin B_{12}	Interaction
Hcy	0.34 ± 0.13	0.33 ± 0.08	0.79 ± 0.49	0.74 ± 0.38	0.0053	0.8286	0.9079
Cys	1.66 ± 0.63	1.8 ± 0.46	2.85 ± 1.4	2.13 ± 0.67	0.0530	0.4447	0.2623
Total GSH	4.94 ± 1.47	5.41 ± 0.46	4.13 ± 1.41	3.29 ± 1.15*	0.0041	0.6975	0.1698
Reduced GSH	3.72 ± 0.97	3.98 ± 0.52	2.98 ± 0.94	2.57 ± 1.05	0.0052	0.8268	0.3451

Data are expressed as means ± S.D. Statistical differences were assessed using a 2-way ANOVA (Bonferroni post hoc test) to examine the effects of meningitis and adjuvant therapy with vitamin B_{12}.
*Statistically significant differences ($P < 0.05$) at Bonferroni post hoc test when compared with the respective sham-infected control (Sh-Sal or Sh-B_{12})
Sh-Sal sham-infected + saline, *Sh-B_{12}* sham-infected + vitamin B_{12}, *Infect-Sal* infected + saline, *Infect-B_{12}* infected + vitamin, *B_{12}Hcy* homocysteine, *Cys* cysteine, *GSH* glutathione

increase in cell methylation capacity [35] in infected animals treated with B_{12}. Results presented in Fig. 3 must be interpreted in light of those shown in Fig. 4, which are explained below.

BM reduced global DNA methylation in the hippocampus, and adjunctive therapy with B_{12} restored this parameter to normal levels

To evaluate the effect of BM and adjuvant therapy with vitamin B_{12} on global DNA methylation in the hippocampus, the %5mC was measured in a colorimetric assay. The percentage of global DNA methylation was reduced by BM ($P < 0.05$), while vitamin B_{12} restored this percentage in infected animals to the control levels (Fig. 4).

Adjunctive therapy with B_{12} counteracted the activation of some inflammatory genes by BM in the hippocampus

Next, the effects of BM and adjuvant therapy with vitamin B_{12} on the expression of selected genes previously implicated in the pathophysiology of BM [12] were assessed by Taqman RT-qPCR. *Ccr2*, *Ccl3,* and *Il1b* had their expression increased by the infection ($P < 0.001$; $P < 0.01$; and $P < 0.001$, respectively); however, unlike other genes tested that were also affected by BM (*Mmp9, Tjp2, Ocln, Timp1, Ccl2, Il6, Casp3, Nfkb, Tnfa, Il10, and Cxcl1*) (Additional file 2), their increased expression was attenuated by adjuvant B_{12} ($P < 0.05$; $P < 0.01$; and $P < 0.01$, respectively) (Fig. 5).

In the infected group treated with B_{12}, Hcy concentration strongly and negatively correlated with *Ccr2* mRNA levels ($r = -1.00$, $P < 0.05$). In the infected group receiving placebo, SAM:SAH ratio inversely correlated with *Ccr2* expression levels ($r = -0.68$, $P < 0.05$), but this correlation was not found in the infected group treated with B_{12}.

Transcription of DNA methyltransferase 3 (*Dnmt3a*) was influenced by the adjuvant therapy, decreasing 1.6-fold in the infected group treated with vitamin B_{12} when

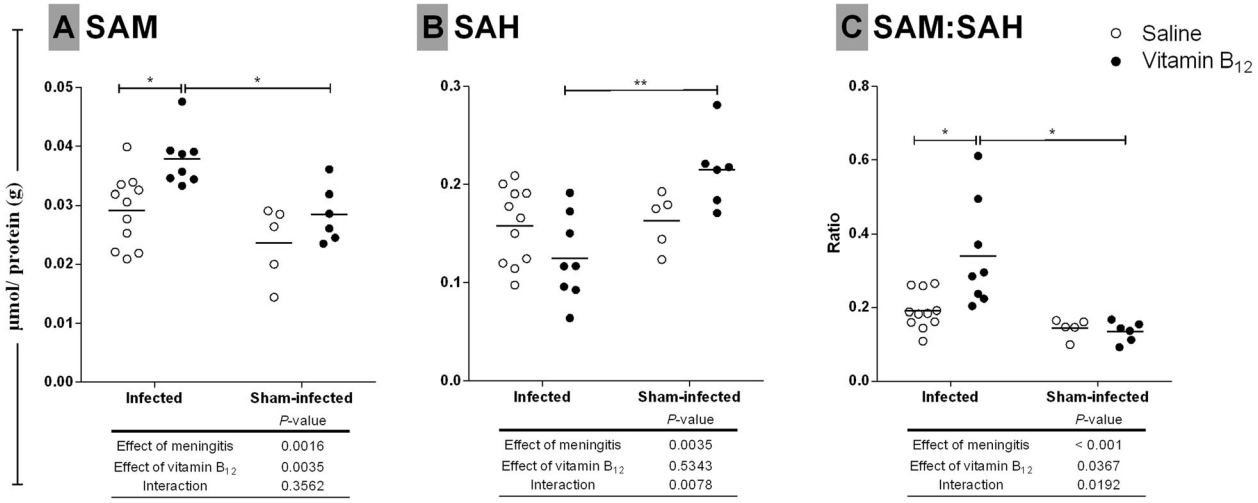

Fig. 3 Effects of BM and adjuvant therapy with vitamin B_{12} on **a** SAM and **b** SAH concentrations and **c** SAM:SAH ratio in the hippocampus. Horizontal bars represent means. The effects of the BM and the vitamin B_{12} adjuvant treatment were compared using a 2-way ANOVA (Bonferroni post hoc test). *P* values in tables below the graphs refer to the 2-way ANOVA and asterisks refer to the post hoc test. *$P < 0.05$; **$P < 0.01$. SAM, *S*-adenosylmethionine; SAH, *S*-adenosylhomocysteine

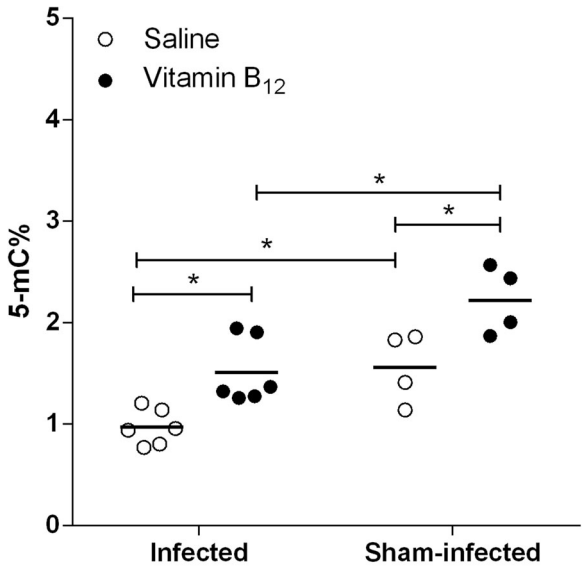

	P-value
Effect of meningitis	< 0.001
Effect of vitamin B_{12}	< 0.001
Interaction	0.6670

Fig. 4 Effects of BM and adjuvant therapy with vitamin B_{12} on the percentage of global DNA methylation (5mC%) in the hippocampus. Horizontal bars represent means. The effects of the BM and the vitamin B_{12} adjuvant therapy were compared using a 2-way ANOVA (Bonferroni post hoc test). *P* values in tables below the graphs refer to the 2-way ANOVA and asterisk refer to the post hoc test. *$P < 0.05$

compared to infected-placebo group ($P < 0.01$) (Fig. 6A). No transcriptional change was observed for the DNA demethylase *Tet1* (Fig. 6B).

Adjunctive therapy with B_{12} induced hypermethylation of CpGs at the promoter of Ccl3 in the hippocampus during BM

To assess whether gene expression during BM was regulated by DNA methylation, differentially methylated regions (DMR) were searched, using a methyl-binding domain-based enrichment approach [36], in the promoter of pro-inflammatory genes *Ccr2, Ccl3*, and *Il1b*, which were upregulated by BM and downregulated by adjuvant therapy with B_{12}. Hypermethylation of CpGs at the promoter region of *Ccl3* was detected in infected animals treated with B_{12} when compared to infected-placebo group ($P < 0.01$) (Figs. 7 and 8).

Discussion

BM induces apoptosis in post mitotic neurons distributed along the dentate gyrus inner granular layer [10, 11], and the damage to the hippocampal formation has been associated with learning and memory impairments among BM survivors [28, 37]. Previous interventional studies with B vitamin supplementation (vitamin B_6, B_{12}, and folate) demonstrated the causal relationship between vitamin B_{12} and cognitive function [38, 39]. In the present study, histomorphological analysis unveiled a significant decrease in apoptotic cell counting in the dentate gyrus inner granular layer of infected animals treated with B_{12}, proving, for the first time, the

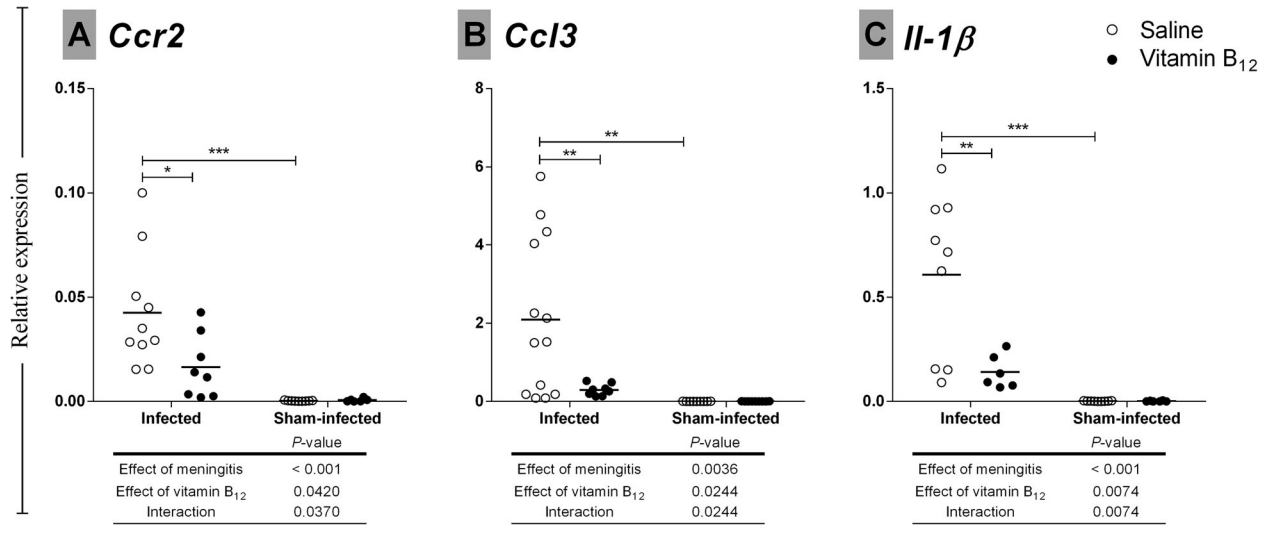

	P-value
Effect of meningitis	< 0.001
Effect of vitamin B_{12}	0.0420
Interaction	0.0370

	P-value
Effect of meningitis	0.0036
Effect of vitamin B_{12}	0.0244
Interaction	0.0244

	P-value
Effect of meningitis	< 0.001
Effect of vitamin B_{12}	0.0074
Interaction	0.0074

Fig. 5 Effects of BM and adjuvant therapy with vitamin B_{12} on hippocampal gene expression *Ccr2, Ccl3*, and *Il1b* mRNA levels in the hippocampus evaluated by the $2^{-\Delta\Delta Ct}$ method. *Rplp2* was used as a reference gene. The effects of BM and vitamin B_{12} were compared using a 2-way ANOVA (Bonferroni post hoc test). *P* values in tables below the graphs refer to the 2-way ANOVA and asterisks refer to the post hoc test. *$P < 0.05$; **$P < 0.01$; ***$P < 0.001$

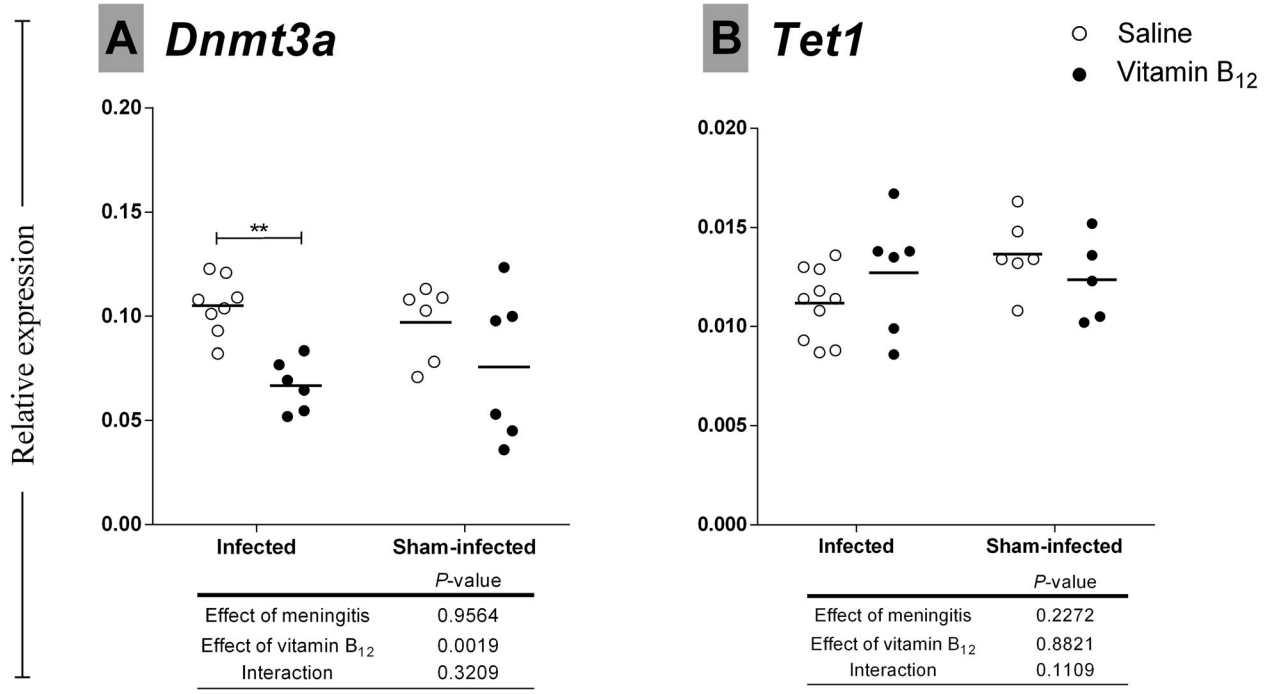

Fig. 6 Effects of BM and adjuvant therapy with vitamin B_{12} on *Dnmt3a and Tet1* expression in the hippocampus. *Dnmt3a and Tet1* mRNA levels in the hippocampus were assessed by the $2^{-\Delta\Delta Ct}$ method. *Ppia* was used as a reference gene. The effects of the BM and vitamin B_{12} were compared using a 2-way ANOVA (Bonferroni post hoc test). *P* values in tables below the graphs refer to the 2-way ANOVA and asterisks refer to the post hoc test. $^{*}P < 0.05$; $^{**}P < 0.01$; $^{***}P < 0.001$

neuroprotective effect of B_{12} as adjuvant therapy to pneumococcal meningitis in the infant rat model (Fig. 2).

B_{12} is a cofactor of methionine synthase, which converts homocysteine into methionine modulating the sulfur amino acid pathway [22]. Our group has previously reported that Hcy concentration is increased in the CSF of children with BM compared to those with enteroviral meningitis or controls without infection in the CNS [26]. In the present study, BM increased hippocampal Hcy levels. Actually, the positive correlation found between hippocampal Hcy concentration and the apoptotic score in the dentate gyrus of infected animals treated with B_{12} supports the hypothesis that an imbalance in the sulfur amino acid homeostasis leading to Hcy accumulation may play a pivotal role in the neurodegenerative process associated to BM. Clinical investigations have shown that Hcy plasma levels are significantly higher in patients with neurologic disorders [40, 41], being a strong independent risk factor for multiple sclerosis [42], Alzheimer's disease [43–47], and Parkinson's disease [45, 48, 49]. Additionally, a tight correlation has been reported between the elevated Hcy plasma levels and cognitive impairment in the elderly [40, 50, 51]. Accumulated evidences show that Hcy is a potent neurotoxin, which contributes to oxidative stress in the brain [47], where it binds and activates *N*-methyl-D-aspartate (NMDA) receptors [52, 53] and mobilizes intracellular calcium stores [54] leading to caspase activation, DNA damage, and neuronal apoptosis in vitro [50, 55, 56] and in vivo [51, 57, 58]. Indeed, it has been reported that Hcy can upregulate *Casp3* and activate caspase 3 via p38-mitogen-activated protein kinase (p38-MAPK) [59]. Although neurotoxicity of Hcy is well documented, this is the first work to directly associate Hcy to the pathophysiology of BM, even though only correlational evidence is provided. Curiously, in the infected group receiving placebo, the apoptotic score did not correlate with Hcy concentration. It is conceivable that, in this group, apoptotic scores are too high to fit within the range where correlation with Hcy concentration occurs.

During acute BM, substrate excess (Hcy) (Table 1) and increased bioavailability of the methionine synthase cofactor (supplemental B_{12}) may have favored Hcy recycling, thus increasing SAM concentration andSAM:SAH ratio (Figs. 1 and 3). During BM, the percentage of global DNA methylation is reduced in the hippocampus, and adjuvant therapy with B12 rescues the normal levels of this parameter, as shown in Fig. 4. SAM:SAH ratio is a well-established indicator of cell methylation capacity [24]. Thus, it is likely that by increasing the SAM:SAH ratio in the hippocampus of infected rats (Fig. 3), adjuvant B12 rescues the normal percentage of global DNA methylation found in sham-infected animals. The

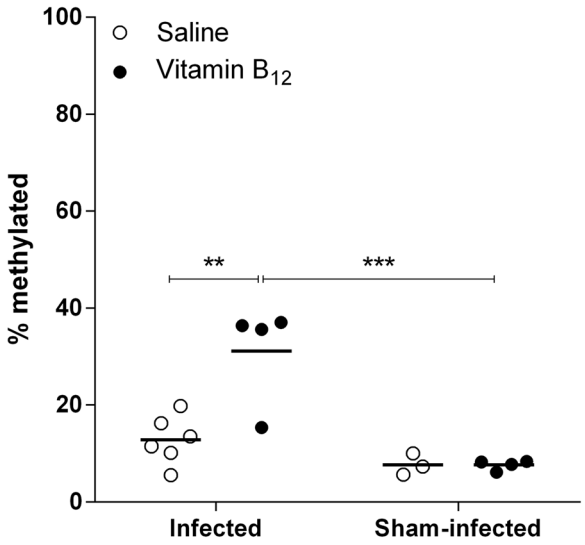

	P-value
Effect of meningitis	$P < 0.001$
Effect of vitamin B_{12}	0.0093
Interaction	0.0092

Fig. 7 Effect of BM and adjuvant therapy with vitamin B_{12} on *Ccl3* gene methylation in the hippocampus. Percentage of methylated DNA in a region covering part of the promotor of *Ccl3* gene. The absolute standard curve method was used to quantify the DNA amount, and data were expressed as a percentage of methylated DNA [(captured DNA/input DNA) × 100]. The effects of BM and vitamin B_{12} were compared using a 2-way ANOVA (Bonferroni post hoc test). *P* values in tables below the graphs refer to the 2-way ANOVA and asterisks refer to the post hoc test. *$P < 0.05$; **$P < 0.01$; ***$P < 0.001$

biological importance of 5-methylcytosine (5mC) as a major epigenetic regulatory mechanism of gene expression has been widely recognized [19]. DNA methylation prevents genomic instability when occurring on interspersed repetitive sequences (IRSs) [60]. Actually, global DNA hypomethylation mostly reflects a decrease in DNA methylation of IRSs, which can cause genome instability [61, 62]. Methyl-deficiency due to a variety of environmental influences causes a global decrease in 5mC content (DNA hypomethylation), which has been proposed as a molecular marker in multiple pathological processes [20]. In addition, oxidative stress facilitates genome-wide hypomethylation [63]. During BM, oxidative DNA damage causes excessive activation of the DNA repair enzyme poly (ADP-ribose) polymerase (PARP). This process comes at a very high energy cost-depleting NAD^+ and ATP, thereby causing apoptosis to the granule cells of the dentate gyrus [64]. However, a link between oxidative DNA damage and global DNA methylation status in the brain during BM had not yet been proposed. The global hypomethylation reported herein in the hippocampal DNA of infected animals may further increase genome instability in the context of BM-induced oxidative stress, which could render granule cells more prone to energy collapse and apoptosis due to PARP hyper-activation. Thus, the neuroprotective effect of adjuvant B_{12} on animals with BM is likely to involve protection against oxidative DNA strand breaks.

DNA methylation also downregulates gene expression when occurring on CpG islands within promoters or other gene regulatory regions [60]. As expected, BM affected the expression of all genes tested [12]. Nevertheless, the *Ccr2*, *Ccl3*, and *Il1b* expression profiles (Fig. 5) were consistent with the hypothesis that treatment with vitamin B_{12} increases the bioavailability of methyl and the methylation of promoters or other regulatory regions of pro-inflammatory genes, leading to their downregulation and, therefore, to the neuroprotection shown in Fig. 2.

When Hcy and B_{12} levels are high, the enzyme methionine synthase can efficiently convert Hcy into methionine, which is then converted into SAM, the methyl donor required for DNA methylation. Accordingly, in the infected group treated with vitamin B_{12}, Hcy

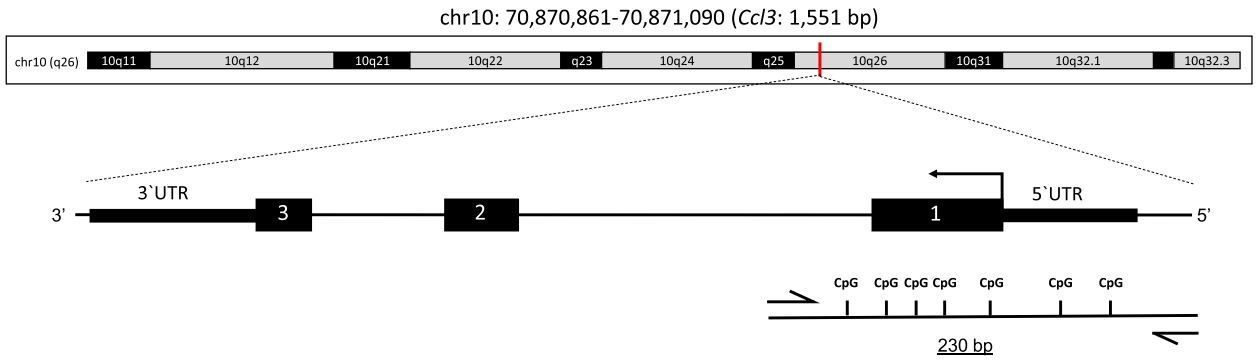

Fig. 8 Schematic representation of *Ccl3* gene. The genome location is chromosome 10 (q26), and the gene encode a protein with 1551 bp. Black arrow, translational start; black boxes, exons; CpG, CG dinucleotides; half arrow, primer pair chosen; dashed line, amplicon region in schematic representation

concentration strongly and negatively correlated with *Ccr2* mRNA levels. It is noteworthy that, in the infected group receiving placebo, SAM:SAH ratio inversely correlated with *Ccr2* expression levels, but this correlation was not found in the infected group treated with B_{12}. In light of these findings, it is reasonable to hypothesize that, below a given threshold, SAM:SAH ratio, which is an indicator of the methylation capacity [24], may determine the methylation level of CpG islands at some regulatory regions of *Ccr2,* downregulating it. However, when SAM:SAH ratio is increased by adjuvant B_{12}, DNA methylation in these CpG islands reaches saturation, gene expression is largely downregulated and correlation is no longer observed.

DNA methyltransferases (DNMTs) transfer the methyl group from SAM to DNA cytosine residues, resulting in a methylated DNA template and SAH, which is recycled to Hcy, as described above. The DNMT family comprises the "maintenance" methyltransferase DNMT1 (which has a preference for hemi-methylated DNA) and the "de novo" catalytic methyltransferases DNMT3A and DNMT3B [65]. Transcription of DNA methyltransferase 3 (*Dnmt3a*) was influenced by the adjuvant therapy ($P < 0.01$), decreasing 1.6-fold in the infected group treated with vitamin B_{12} when compared to infected-placebo group (Fig. 6A). This result suggests a negative-feedback loop in response to the excess of substrate (SAM) in the infected rats receiving B_{12}. No transcriptional change due to BM or B_{12} was observed in the DNA demethylase *Tet1* (Fig. 6B), which catalyzes the conversion of 5mC into 5-hydroxymethylcytosine (5hmC) and plays a key role in active DNA demethylation [66]. Post-transcriptional or post-translational regulation of Tet1 in response to BM of adjuvant B_{12} cannot be discarded.

To assess whether gene expression during BM is regulated by DNA methylation, differentially methylated regions (DMR) were searched, using a methyl-binding domain-based enrichment approach [36], at the promoter of pro-inflammatory genes *Ccr2, Ccl3* and *Il1b,* which were upregulated by BM and downregulated by adjuvant therapy with B_{12} (Fig. 5). Hypermethylation of CpG islands at the promoter region of *Ccl3* was detected in infected animals treated with B_{12} (Figs. 7 and 8), proving the hypothesis that the mode of action of this potential neuroprotective adjuvant therapy to BM involves methyl-dependent epigenetic mechanisms of gene regulation. Unfortunately, regional DNA sequence constraints impeded the screening by qPCR of other CpG islands in the selected genes. More robust approaches such as bisulfite conversion followed by genome-wide DNA sequencing will be of great value to unveil the ensemble of genes playing a role in the pathophysiology of BM and which regulation involves DNA methylation, susceptible to be modulated by adjuvant therapy with B_{12}.

The activity score assessed at 18 h after intracysternal inoculation with pneumococci (and before the second dose of B12) is a rough measure of the clinical state of the infant rats that mostly indicates inflammation in the CNS. TNF-α, IL-1β, and IL-6 are the major pro-inflammatory cytokines with early response in pneumococcal meningitis [67]. From these inflammatory mediators, only IL-1β was downregulated by adjuvant therapy with B12 in infected rats. Thus, it is unlikely that B12 might improve the overall clinical state of rats at such an early timepoint.

Conclusions

Overall, the results of this work support the hypothesis that the imbalance caused by BM in the sulfur amino acid homeostasis, which leads to Hcy accumulation in the hippocampus, may play a pivotal role in inducing apoptosis in the progenitor cells and post mitotic neurons in the hippocampal dentate gyrus. The BM-associated decrease in global DNA methylation probably contributes to genomic instability and to the previously reported over activation of PARP, a NAD-consuming DNA repair enzyme. Furthermore, adjuvant therapy with vitamin B_{12} modulates the Hcy pathway, increasing global DNA methylation, which may contribute to its neuroprotective effect on the infant rat model of BM either by reducing genome instability and by modulating the expression of critical genes to the pathophysiology of this disease.

Supplementary information

Supplementary information accompanies this paper at https://doi.org/10.1186/s12974-020-01763-y.

Additional file 1. Experimental design. Diagrammatic representation of the experimental design of this study.

Additional file 2. Effects of BM and adjuvant therapy with vitamin B12 on gene expression in the hippocampus. Table showing the expression patterns of 11 genes previously implicated in the pathophysiology of pneumococcal meningitis that were not regulated by adjuvant therapy with vitamin B_{12}.

Abbreviations

%5mC: Percentage of methylated DNA; 5hmC: 5-hydroxymethylcytosine; 5mC: 5-methylcytosine; BM: Bacterial meningitis; CNS: Central nervous system; CSF: Cerebrospinal fluid; Ct: Cycle thresholds; CX: Cortex; Cys: Cysteine; DMR: Differentially methylated regions; DNMTs: DNA methyltransferases; GSH: Glutathione; HC: Hippocampus; Hcy: Homocysteine; Hib: *Haemophilus influenzae* type b; HPLC: High-performance liquid chromatography; IRSs: Interspersed repetitive sequences; NMDA: *N*-methyl-D-aspartate; OD: Optical density; PARP: DNA repair enzyme poly (ADP-ribose) polymerase; PBS: Phosphate-buffered saline; SAH: *S*-adenosylhomocysteine (AdoHcy); SAM: *S*-adenosylmethionine (AdoMet)

Acknowledgements

Not applicable.

Authors' contributions

KBQ participated in the experiments with the animal model, analyzed and interpreted data regarding molecular biology, and contributed to the writing of the manuscript. VC-S and VD'A analyzed and interpreted the data

regarding the sulfur amino acid assays. FLA participated in the conception and interpretation of the experiment to assess the methylation status of candidate genes. GAR participated in the study conception, data interpretation, and manuscript writing. RSC conceived the study; analyzed and interpreted the data regarding the animal model, histology, molecular biology, and sulfur amino acid assays; and wrote the manuscript. All authors critically reviewed the manuscript. The authors read and approved the final manuscript.

Funding
This work was supported by Inova Fundação Oswaldo Cruz (FIOCRUZ). The funding body had no role in the design of the study, collection, analysis, and interpretation of data and in writing of the manuscript.

Availability of data and materials
All data generated or analyzed during this study are included in this published article.

Ethics approval and consent to participate
All of the experimental procedures were approved by the Ethics Committee of Care and Use of Laboratory Animals (CEUA-FIOCRUZ, protocol LW-23/17) and were conducted in accordance with the regulations described in the Committee's Guiding Principles Manual.

Consent for publication
Not applicable.

Competing interests
The authors declare that they have no competing interests.

Author details
[1]Neurogenômica/Imunopatologia, Instituto René Rachou (IRR), Fundação Oswaldo Cruz (FIOCRUZ), Av. Augusto de Lima, 1715, Belo Horizonte, MG CEP 30190-002, Brazil. [2]Departamento de Psicobiologia, Escola Paulista de Medicina, Universidade Federal de São Paulo (UNIFESP-EPM), Rua Botucatu, 740, São Paulo, SP CEP 04023-062, Brazil. [3]Faculdade de Medicina Veterinária de Araçatuba, Universidade Estadual Paulista (UNESP), R. Clóvis Pestana, 793, Araçatuba, SP CEP 16050-680, Brazil. [4]Laboratório de Pesquisa em Bacteriologia, Departamento de Propedêutica Complementar, Faculdade de Medicina, Universidade Federal de Minas Gerais (UFMG), Av. Prof. Alfredo Balena, 190, Belo Horizonte, MG CEP 30130-100, Brazil.

Received: 25 October 2019 Accepted: 27 February 2020
Published online: 01 April 2020

References

1. Brouwer MC, van de Beek D. Epidemiology of community-acquired bacterial meningitis. Curr Opin Infect Dis. 2018;31:78–84.
2. Schuchat A, Robinson K, Wenger J, Harrison L, Farley M, Reingold A, Lefkowitz L, Perkins B. Bacterial meningitis in the United States in 1995. Active surveillance team. N Engl J Med. 1997;337:970–6.
3. Molyneux E, Walsh A, Phiri A, Molyneux M. Acute bacterial meningitis in children admitted to the Queen Elizabeth Central Hospital, Blantyre, Malawi in 1996-97. Tropical Med Int Health. 1998;3:610–8.
4. Scheld W, Koedel U, Nathan B, Pfister H. Pathophysiology of bacterial meningitis: mechanism(s) of neuronal injury. J Infect Dis. 2002;186(Suppl 2): S225–33.
5. Bedford H, de Louvois J, Halket S, Peckham C, Hurley R, Harvey D. Meningitis in infancy in England and Wales: follow up at age 5 years. BMJ. 2001;323:533–6.
6. Merkelbach S, Sittinger H, Schweizer I, Muller M. Cognitive outcome after bacterial meningitis. Acta Neurol Scand. 2000;102:118–23.
7. Dawson K, Emerson J, Burns J. Fifteen years of experience with bacterial meningitis. Pediatr Infect Dis J. 1999;18:816–22.
8. Grimwood K, Anderson P, Anderson V, Tan L, Nolan T. Twelve year outcomes following bacterial meningitis: further evidence for persisting effects. Arch Dis Child. 2000;83:111–6.
9. Meli D, Christen S, Leib S, Tauber M. Current concepts in the pathogenesis of meningitis caused by *Streptococcus pneumoniae*. Curr Opin Infect Dis. 2002;15:253–7.
10. Bifrare Y, Gianinazzi C, Imboden H, Leib S, Tauber M. Bacterial meningitis causes two distinct forms of cellular damage in the hippocampal dentate gyrus in infant rats. Hippocampus. 2003;13:481–8.
11. Grandgirard D, Bifrare Y, Pleasure S, Kummer J, Leib S, Tauber M. Pneumococcal meningitis induces apoptosis in recently postmitotic immature neurons in the dentate gyrus of neonatal rats. Dev Neurosci. 2007;29:134–42.
12. Coimbra R, Voisin V, de Saizieu A, Lindberg R, Wittwer M, Leppert D, Leib S. Gene expression in cortex and hippocampus during acute pneumococcal meningitis. BMC Biol. 2006;4:15.
13. McEwen BS. Physiology and neurobiology of stress and adaptation: central role of the brain. Physiol Rev. 2007;87:873–904.
14. McEwen BS. Mood disorders and allostatic load. Biol Psychiatry. 2003;54: 200–7.
15. Conrad CD. Chronic stress-induced hippocampal vulnerability: the glucocorticoid vulnerability hypothesis. Rev Neurosci. 2008;19:395–411.
16. Weaver IC, Cervoni N, Champagne FA, D'Alessio AC, Sharma S, Seckl JR, Dymov S, Szyf M, Meaney MJ. Epigenetic programming by maternal behavior. Nat Neurosci. 2004;7:847–54.
17. Sokolova NE, Shiryaeva NV, Dyuzhikova NA, Savenko YN, Vaido AI. Effect of long-term mental and pain stress on the dynamics of H4 histone acetylation in hippocampal neurons of rats with different levels of nervous system excitability. Bull Exp Biol Med. 2006;142:341–3.
18. Chandramohan Y, Droste SK, Reul JM. Novelty stress induces phospho-acetylation of histone H3 in rat dentate gyrus granule neurons through coincident signalling via the *N*-methyl-D-aspartate receptor and the glucocorticoid receptor: relevance for c-fos induction. J Neurochem. 2007; 101:815–28.
19. Rodriguez-Dorantes M, Tellez-Ascencio N, Cerbon MA, Lopez M. Cervantes a: [DNA methylation: an epigenetic process of medical importance]. Rev Investig Clin. 2004;56:56–71.
20. Jaenisch R, Bird A. Epigenetic regulation of gene expression: how the genome integrates intrinsic and environmental signals. Nat Genet. 2003; 33(Suppl):245–54.
21. Pfalzer AC, Choi SW, Tammen SA, Park LK, Bottiglieri T, Parnell LD, Lamon-Fava S. *S*-adenosylmethionine mediates inhibition of inflammatory response and changes in DNA methylation in human macrophages. Physiol Genomics. 2014;46:617–23.
22. Tehlivets O, Malanovic N, Visram M, Pavkov-Keller T, Keller W. *S*-adenosyl-L-homocysteine hydrolase and methylation disorders: yeast as a model system. Biochim Biophys Acta. 1832;2013:204–15.
23. Esse R, Florindo C, Imbard A, Rocha MS, de Vriese AS, Smulders YM, Teerlink T, Tavares de Almeida I, Castro R, Blom HJ. Global protein and histone arginine methylation are affected in a tissue-specific manner in a rat model of diet-induced hyperhomocysteinemia. Biochim Biophys Acta. 2013;1832: 1708–14.
24. Chen NC, Yang F, Capecci LM, Gu Z, Schafer AI, Durante W, Yang XF, Wang H. Regulation of homocysteine metabolism and methylation in human and mouse tissues. FASEB J. 2010;24:2804–17.
25. Huang T, Li K, Asimi S, Chen Q, Li D. Effect of vitamin B-12 and n-3 polyunsaturated fatty acids on plasma homocysteine, ferritin, C-reaction protein, and other cardiovascular risk factors: a randomized controlled trial. Asia Pac J Clin Nutr. 2015;24:403–11.
26. Coimbra RS, Calegare BF, Candiani TM, D'Almeida V. A putative role for homocysteine in the pathophysiology of acute bacterial meningitis in children. BMC Clin Pathol. 2014;14:43.
27. Leib SL, Clements JM, Lindberg RL, Heimgartner C, Loeffler JM, Pfister LA, Tauber MG, Leppert D. Inhibition of matrix metalloproteinases and tumour necrosis factor alpha converting enzyme as adjuvant therapy in pneumococcal meningitis. Brain. 2001;124:1734–42.
28. Loeffler JM, Ringer R, Hablutzel M, Tauber MG, Leib SL. The free radical scavenger alpha-phenyl-tert-butyl nitrone aggravates hippocampal apoptosis and learning deficits in experimental pneumococcal meningitis. J Infect Dis. 2001;183:247–52.
29. Gianinazzi C, Grandgirard D, Imboden H, Egger L, Meli DN, Bifrare YD, Joss PC, Tauber MG, Borner C, Leib SL. Caspase-3 mediates hippocampal apoptosis in pneumococcal meningitis. Acta Neuropathol. 2003;105:499–507.
30. Blaise S, Alberto JM, Nédélec E, Ayav A, Pourié G, Bronowicki JP, Guéant JL, Daval JL. Mild neonatal hypoxia exacerbates the effects of vitamin-deficient diet on homocysteine metabolism in rats. Pediatr Res. 2005;57:777–82.

31. Pfeiffer C, Huff D, Gunter E. Rapid and accurate HPLC assay for plasma total homocysteine and cysteine in a clinical laboratory setting. Clin Chem. 1999; 45:290–2.
32. Galdieri LC, Arrieta SR, Silva CM, Pedra CA, D'Almeida V. Homocysteine concentrations and molecular analysis in patients with congenital heart defects. Arch Med Res. 2007;38:212–8.
33. Livak KJ, Schmittgen TD. Analysis of relative gene expression data using real-time quantitative PCR and the 2(-Delta Delta C(T)) method. Methods. 2001;25:402–8.
34. Pieper RO, Patel S, Ting SA, Futscher BW, Costello JF. Methylation of CpG island transcription factor binding sites is unnecessary for aberrant silencing of the human MGMT gene. J Biol Chem. 1996;271:13916–24.
35. Caudill MA, Wang JC, Melnyk S, Pogribny IP, Jernigan S, Collins MD, Santos-Guzman J, Swendseid ME, Cogger EA, James SJ. Intracellular *S*-adenosylhomocysteine concentrations predict global DNA hypomethylation in tissues of methyl-deficient cystathionine beta-synthase heterozygous mice. J Nutr. 2001;131:2811–8.
36. Aberg KA, Xie L, Chan RF, Zhao M, Pandey AK, Kumar G, Clark SL, van den Oord EJ. Evaluation of methyl-binding domain based enrichment approaches revisited. PLoS One. 2015;10:e0132205.
37. Koedel U, Scheld WM, Pfister HW. Pathogenesis and pathophysiology of pneumococcal meningitis. Lancet Infect Dis. 2002;2:721–36.
38. de Jager CA, Oulhaj A, Jacoby R, Refsum H, Smith AD. Cognitive and clinical outcomes of homocysteine-lowering B-vitamin treatment in mild cognitive impairment: a randomized controlled trial. Int J Geriatr Psychiatry. 2012;27: 592–600.
39. Walker JG, Batterham PJ, Mackinnon AJ, Jorm AF, Hickie I, Fenech M, Kljakovic M, Crisp D, Christensen H. Oral folic acid and vitamin B-12 supplementation to prevent cognitive decline in community-dwelling older adults with depressive symptoms--the Beyond Ageing Project: a randomized controlled trial. Am J Clin Nutr. 2012;95:194–203.
40. Baydas G, Kutlu S, Naziroglu M, Canpolat S, Sandal S, Ozcan M, Kelestimur H. Inhibitory effects of melatonin on neural lipid peroxidation induced by intracerebroventricularly administered homocysteine. J Pineal Res. 2003;34: 36–9.
41. Ansari R, Mahta A, Mallack E, Luo JJ. Hyperhomocysteinemia and neurologic disorders: a review. J Clin Neurol. 2014;10:281–8.
42. Russo C, Morabito F, Luise F, Piromalli A, Battaglia L, Vinci A, Trapani Lombardo V, de Marco V, Morabito P, Condino F, et al. Hyperhomocysteinemia is associated with cognitive impairment in multiple sclerosis. J Neurol. 2008;255:64–9.
43. Clarke R, Smith AD, Jobst KA, Refsum H, Sutton L, Ueland PM. Folate, vitamin B12, and serum total homocysteine levels in confirmed Alzheimer disease. Arch Neurol. 1998;55:1449–55.
44. Morris MS. Homocysteine and Alzheimer's disease. Lancet Neurol. 2003;2: 425–8.
45. Genedani S, Rasio G, Cortelli P, Antonelli F, Guidolin D, Galantucci M, Fuxe K, Agnati LF. Studies on homocysteine and dehydroepiandrosterone sulphate plasma levels in Alzheimer's disease patients and in Parkinson's disease patients. Neurotox Res. 2004;6:327–32.
46. Agnati LF, Genedani S, Rasio G, Galantucci M, Saltini S, Filaferro M, Franco R, Mora F, Ferre S, Fuxe K. Studies on homocysteine plasma levels in Alzheimer's patients. Relevance for neurodegeneration. J Neural Transm (Vienna). 2005;112:163–9.
47. Cankurtaran M, Yesil Y, Kuyumcu ME, Ozturk ZA, Yavuz BB, Halil M, Ulger Z, Cankurtaran ES, Ariogul S. Altered levels of homocysteine and serum natural antioxidants links oxidative damage to Alzheimer's disease. J Alzheimers Dis. 2013;33:1051–8.
48. Kuhn W, Roebroek R, Blom H, van Oppenraaij D, Przuntek H, Kretschmer A, Buttner T, Woitalla D, Muller T. Elevated plasma levels of homocysteine in Parkinson's disease. Eur Neurol. 1998;40:225–7.
49. Smeyne M, Smeyne RJ. Glutathione metabolism and Parkinson's disease. Free Radic Biol Med. 2013;62:13–25.
50. Zhao H, Ji ZH, Liu C, Yu XY. Neuroprotection and mechanisms of atractylenolide III in preventing learning and memory impairment induced by chronic high-dose homocysteine administration in rats. Neuroscience. 2015;290:485–91.
51. Wang J, Bai X, Chen Y, Zhao Y, Liu X. Homocysteine induces apoptosis of rat hippocampal neurons by inhibiting 14-3-3epsilon expression and activating calcineurin. PLoS One. 2012;7:e48247.
52. Murphy TH, Miyamoto M, Sastre A, Schnaar RL, Coyle JT. Glutamate toxicity in a neuronal cell line involves inhibition of cystine transport leading to oxidative stress. Neuron. 1989;2:1547–58.
53. Schubert D, Piasecki D. Oxidative glutamate toxicity can be a component of the excitotoxicity cascade. J Neurosci. 2001;21:7455–62.
54. Lipton SA, Kim WK, Choi YB, Kumar S, D'Emilia DM, Rayudu PV, Arnelle DR, Stamler JS. Neurotoxicity associated with dual actions of homocysteine at the *N*-methyl-D-aspartate receptor. Proc Natl Acad Sci U S A. 1997;94:5923–8.
55. Yeganeh F, Nikbakht F, Bahmanpour S, Rastegar K, Namavar R. Neuroprotective effects of NMDA and group I metabotropic glutamate receptor antagonists against neurodegeneration induced by homocysteine in rat hippocampus: in vivo study. J Mol Neurosci. 2013;50:551–7.
56. Jang Y, Kim J, Ko JW, Kwon YH. Homocysteine induces PUMA-mediated mitochondrial apoptosis in SH-SY5Y cells. Amino Acids. 2016;48:2559–69.
57. Wei HJ, Xu JH, Li MH, Tang JP, Zou W, Zhang P, Wang L, Wang CY, Tang XQ. Hydrogen sulfide inhibits homocysteine-induced endoplasmic reticulum stress and neuronal apoptosis in rat hippocampus via upregulation of the BDNF-TrkB pathway. Acta Pharmacol Sin. 2014;35:707–15.
58. Ovey IS, Naziroglu M. Homocysteine and cytosolic GSH depletion induce apoptosis and oxidative toxicity through cytosolic calcium overload in the hippocampus of aged mice: involvement of TRPM2 and TRPV1 channels. Neuroscience. 2015;284:225–33.
59. Shastry S, Ingram AJ, Scholey JW, James LR. Homocysteine induces mesangial cell apoptosis via activation of p38-mitogen-activated protein kinase. Kidney Int. 2007;71:304–11.
60. Tirado-Magallanes R, Rebbani K, Lim R, Pradhan S, Benoukraf T. Whole genome DNA methylation: beyond genes silencing. Oncotarget. 2017;8: 5629–37.
61. Chen RZ, Pettersson U, Beard C, Jackson-Grusby L, Jaenisch R. DNA hypomethylation leads to elevated mutation rates. Nature. 1998;395:89–93.
62. Zheng Y, Joyce BT, Liu L, Zhang Z, Kibbe WA, Zhang W, Hou L. Prediction of genome-wide DNA methylation in repetitive elements. Nucleic Acids Res. 2017;45:8697–711.
63. Patchsung M, Boonla C, Amnattrakul P, Dissayabutra T, Mutirangura A, Tosukhowong P. Long interspersed nuclear element-1 hypomethylation and oxidative stress: correlation and bladder cancer diagnostic potential. PLoS One. 2012;7:e37009.
64. Koedel U, Winkler F, Angele B, Fontana A, Pfister H. Meningitis-associated central nervous system complications are mediated by the activation of poly(ADP-ribose) polymerase. J Cereb Blood Flow Metab. 2002;22:39–49.
65. Jurkowska RZ, Jurkowski TP, Jeltsch A. Structure and function of mammalian DNA methyltransferases. Chembiochem. 2011;12:206–22.
66. Williams K, Christensen J, Pedersen MT, Johansen JV, Cloos PA, Rappsilber J, Helin K. TET1 and hydroxymethylcytosine in transcription and DNA methylation fidelity. Nature. 2011;473:343–8.
67. Mook-Kanamori BB, Geldhoff M, van der Poll T, van de Beek D. Pathogenesis and pathophysiology of pneumococcal meningitis. Clin Microbiol Rev. 2011; 24:557–91.

Publisher's Note